Heterogeneous & Homogeneous & Bio- & Nano-

CHEMCATCHEM

CATALYSIS

Title: Kinetics of the Homogeneous and Heterogeneous Coupling of Furfural with Biomass-derived Alcohols

Authors: Konstantinos Antonios Goulas and Amit A Gokhale

To be cited as: *ChemCatChem* 10.1002/cctc.201701866

Link to VoR: http://dx.doi.org/10.1002/cctc.201701866

WILEY-VCH

www.chemcatchem.org

A Journal of ChemPubSoc Europe

WILEY-VCH

Kinetics of the Homogeneous and Heterogeneous Coupling of Furfural with Biomass-derived Alcohols

Konstantinos A. Goulas*[a,b] Amit A. Gokhale[a,c]

Abstract: The tandem dehydrogenation and aldol condensation of butanol with furfural was investigated over homogeneous and heterogeneous catalysts using kinetics and isotope effects. In the homogeneous system, Ni(dppe)Cl_2 catalyzes the transfer dehydrogenation of butanol to the furfural, while the aldol condensation of butyraldehyde and furfural takes place over the basic K_2CO_3 cocatalyst. In the heterogeneous system, a transition-metal-free mixed Mg-Al oxide, both the transfer hydrogenation and aldol condensation take place over the basic sites of the catalyst, with the rate-determining step being the alpha-hydride transfer from the butanol to the furfural.

Introduction

It has now been well established that the rise in atmospheric CO_2 levels over the last two centuries have led to global warming. In both, the developed and developing economies, the transportation sector contributes significant proportion of the overall greenhouse gas (GHG) emissions. Therefore, reduction of GHG emissions, primarily CO_2, from the transportation sector is a cornerstone in our quest to mitigate the impacts of climate change. To attain this goal, the incorporation of renewable fuels, such as those derived from biomass, into the fuels value chain is necessary as part of a move to a sustainable economy. Many of the processes for conversion of biomass into fuels or chemicals often employ chemical catalysis[1] or fermentation[2] as an intermediate step to obtain platform molecules. Some platform molecules that have garnered attention are the C_5 and C_6 sugar-derived aldehydes such as furfural and 5-hydroxymethylfurfural, which can be produced using homogeneous[1a, 3] or heterogeneous catalysis.[4] Similarly, fermentation of sugars can yield short-chain alcohols,[5] ketones[6] and carboxylic acids[7] which may also be used as platform molecules.

The synthesis of high value-added fuels, such as diesel (C_{13}-C_{26}) and jet fuel (C_9-C_{14}), from platform molecules requires the formation of new C-C bonds, as most platform molecules are in the C_2-C_6 range.[8] In these efforts, researchers have reported the use of acidic catalysts to form C-C bonds between alkylfurans and aldehydes,[9] and the use of basic catalysts for the aldol condensation of aldehydes and ketones to longer-chain molecules.[10] Subsequent hydrodeoxygenation of these species affords alkanes and cycloalkanes that can be directly blended with petroleum-derived fuels.[11] Basic catalysts have also been used to increase the carbon chain length, via aldol condensation reactions. Among other molecules, acetone,[6, 12] cyclopentanone[13] and angelica lactone[14] have been used to provide acidic protons that can undergo enolization and subsequent C-C bond formation to give long-chain alkanes after hydrodeoxygenation.[15]

In the recent years, alkylation of furan and furfural, to produce chemicals and fuels has also been an area of increased interest. For example Koehle et al. reported on the acylation of furans with acetic anhydride over acidic zeolites and the subsequent hydrodeoxygenation of the products to form precursors to p-methylstyrene and p-divinylbenzene.[16] Park et al. reported on the synthesis of long-chain alkylfurans using lauric acid and trifluoroacetic anhydride, and their subsequent sulfonation to form renewable surfactants.[17] By employing homogeneous and heterogeneous Ni-based catalysts, in a previous work, our group showed that water-sensitive anhydrides are unnecessary in the aldol condensation of furfural with biomass-derived alcohols to form unsaturated long-chain furylaldehydes (Scheme 1). Subsequent hydrodeoxygenation reactions form the desired gasoline, jet and diesel-range blendstocks. Based on life-cycle analysis, this approach was reported to achieve net greenhouse gas decreases of 53% to 79%, compared to conventional fuels.[18]

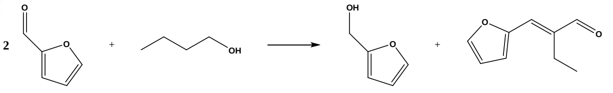

1

Scheme 1. Reaction of furfural with butanol to form furfuryl alcohol and the unsaturated aldehyde 1.

While industrial scale-up of the heterogeneous systems perhaps makes more sense, this is a unique system where both homogeneous as well as heterogenous catalysis seem to work quite well but most likely follow different mechanisms. In order to compare the relative advantages of heterogeneous and homogeneous catalysis, kinetic studies are quite useful and with that motivation, we undertook this study to better understand the condensation of furfural with alcohols. In this work, liquid-phase and gas-phase kinetic experiments were carried out, in combination with kinetic isotope effect investigations to propose a mechanism for the homogeneous and heterogeneous furfural condensation with aliphatic alcohols.

---

[a] Dr. K. A. Goulas, Dr. A. A. Gokhale
Energy Biosciences Institute
University of California, Berkeley
Berkeley, CA 94720, USA
E-mail: goulas@udel.edu
[b] Dr. K. A. Goulas,
Catalysis Center for Energy Innovation
University of Delaware
Newark, DE 19711, USA
[c] Dr. A. A. Gokhale
BASF Corporation
Iselin, NJ 08830, USA

Supporting information for this article is given via a link at the end of the document.

10.1002/cctc.201701866

Results and Discussion

First, the kinetics of the furfural-butanol coupling reaction over the Ni(dppe)Cl_2 catalyst and K_2CO_3 co-catalyst were investigated in the liquid phase. This study revealed an induction period over the first two hours of reaction (Figure 1). During this phase of the reaction, no addition product **1** was formed, but butanol was consumed. This suggests that some intermediate must be formed during the induction phase. One possibility for the intermediate is an active form of the catalyst obtained via replacement of Cl- ligands with butoxide. Such a mechanism would consume 10% of the butanol from our reaction mixture. However, we find that close to 20% of butanol is consumed by the end of the induction period. While this does not negate the possibility of Cl^- ligand replacement, it strongly suggests that the intermediate is a species along the reaction pathway. Incidentally, this is also consistent with the formation of butyraldehyde observed by GC during the induction period.

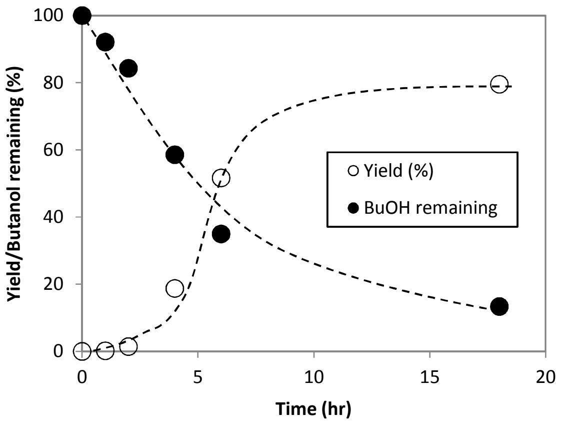

Figure 1. Liquid-phase reaction progress study of the addition of butanol to furfural. 1 mmol butanol, 2 mmol furfural, 1 mL toluene, 413 K. 26.4 mg Ni(dppe)Cl_2, 49.6 mg K_2CO_3. Dashed lines represent qualitative trends.

Control experiments indicate that no reaction was observed with butanol and furfural in the absence of the Ni complex, suggesting that its primary role lies in the dehydrogenation of the butanol (Table 1). Consistent with earlier reports,[19] the condensation of the furfural with the butyraldehyde proceeded readily over K_2CO_3, both in the presence and the absence of Ni.

It is known that radical mechanisms can be involved in nickel-catalyzed reactions[20]. In order to test the possibility of radical intermediates being involved in the butanol dehydrogenation reaction, a radical inhibitor was added to the reaction (butylated hydroxytoluene-BHT). A negligible reduction of the yield was observed, compared to the reaction in the absence of BHT. This observation suggests that a radical mechanism can be ruled out.

Table 1. Control experiments for the condensation of furfural with butanol over Ni(dppe)Cl_2 and K_2CO_3. 1 mmol C_4 aliphatic oxygenates, 2 mmol furfural, 413 K, toluene solvent.

Catalyst	Reactants	Yield **1** (%)	C4 conversion
Ni(dppe)Cl_2, K_2CO_3	Butanol, furfural	79	88
Ni(dppe)Cl_2, K_2CO_3	Butyraldehyde, furfural	81	100
Ni(dppe)Cl_2, K_2CO_3	Butanol, furfural, BHT	78	85
K_2CO_3	Butyraldehyde, furfural	77	100
K_2CO_3	Butanol, furfural	10	22

The direct dehydrogenation of butanol to butyraldehyde and hydrogen via a metal hydride-mediated mechanism was investigated. Such mechanisms have also been invoked as intermediates for the dehydrogenation of alcohols to aldehydes[21] and are the dominant mechanism of alcohol dehydrogenation over heterogeneous catalysts. Moreover, Ni complexes are known to form hydrides. In order to investigate the possibility of Ni hydrides being intermediates of the reaction, the headspace of the reaction was sampled and analyzed using GC/TCD. The absence of hydrogen gas in this experiment is an indication that a hydride mechanism is not active in this reaction. Instead of a Ni-hydride mechanism, we propose that the Ni complex acts as a Lewis acid[22] to coordinate the furfural, which receives a hydride from a Ni n-butoxide intermediate. Such butoxides may be formed by the deprotonation of alcohol by the base (K_2CO_3) and the substitution of one or two chloride ligands on the Ni.

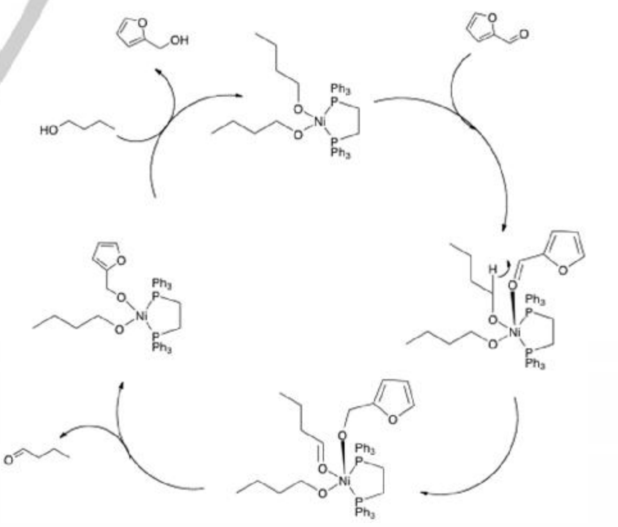

Scheme 2. Proposed mechanism of dehydrogenation of butanol to butyraldehyde via hydride transfer to furfural.

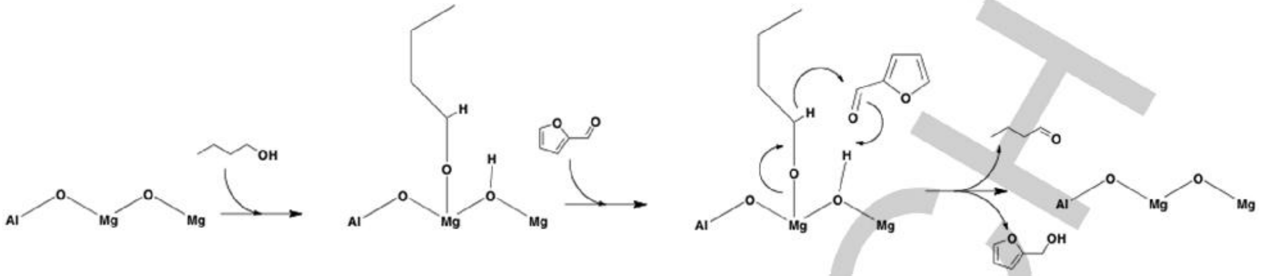

Scheme 3. Proposed mechanism of transfer hydrogenation over a basic catalyst.

No butanol was converted to butyraldehyde in the absence of furfural. This, combined with the observation (Figure 2) that the butanol consumption rate in the induction period was proportional to the furfural concentration is further evidence of the existence of a transfer hydrogenation mechanism. These observations suggest that the rate-determining step of the catalytic cycle, as depicted in scheme 2, is the transfer of the hydride from the butoxide to the furfural. This transfer is plausible, as it can occur via a favorable six-member transition state.

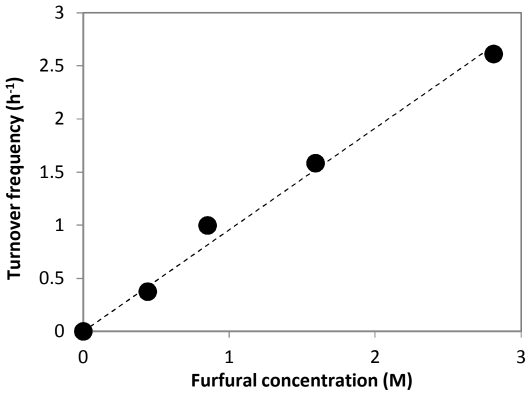

Figure 2. Rate of butanol dehydrogenation as a function of furfural concentration. 0.05 mmol Ni(dppe)Cl_2, 0.3 mmol K_2CO_3, 413 K, C_{BuOH} = 1 M.

Heterogeneous catalysts are generally preferred in the industry to homogeneous ones, as they are generally more robust and easier to handle. For this reason, the heterogenization of the reaction was investigated by combining a Ni^{2+} material with a basic support, by synthesizing a Ni-MgO-Al_2O_3 catalyst from a Ni-substituted hydrotalcite precursor. Hydrotalcites and the oxides derived thereof have found extensive use in many biomass-related applications.[22] A gas-phase reaction system was selected to probe the reaction, in order to obtain higher accuracy measurements at differential conditions and also with the end goal of using a two-bed reactor system to carry out the condensation and the hydrodeoxygenation reactions. We synthesized a range of materials with different Ni weight loadings, in order to probe the effect of Ni and to optimize the catalyst.

Table 2. Textural properties of heterogeneous catalysts.

Catalyst	Surface Area (m^2 g^{-1})	Ni content (wt. %)
HT	221	0
Ni10HT	212	9.6
Ni20HT	248	5.6
Ni40HT	216	2.8

Figure 3 shows the effects of the Ni loading on the reaction rates. Remarkably, both the aldol condensation rate and the dehydrogenation rate decreased with increasing Ni loading on the catalyst, reducing by about 50% from 0% Ni to 9.6% Ni. This is not due to changes in the surface area or the crystal structure of the catalyst, as all catalysts have surface areas from 210 to 250 m^2 g^{-1} (Table 2) and are mostly cubic periclase-like solids (Figure 4),[23] with minor contributions from a mostly amorphous Mg-Al oxyhydroxide, as evidenced by the broad peak around 32°.[24] Instead, this shows that in the heterogeneous system, Ni is not required for the reaction to take place. On the contrary, the presence of Ni seems to be detrimental to the reaction. The reason for this could be that both hydrogenation and aldol condensation reactions take place over basic sites, the strength and number of which has been shown to be reduced upon substitution of Mg^{2+} by Ni^{2+}.[25] Basic solids are known to catalyze the dehydrogenation of alcohols via a hydride transfer to a carbonyl group and a mechanism like this could be in play here as well.[26] Therefore, in order to probe this hypothesis, a set of kinetic experiments was performed in the flow reactor.

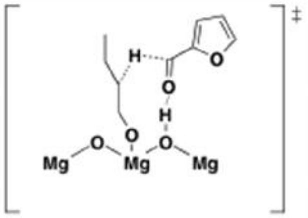

Scheme 4. Proposed mechanism of dehydrogenation of butanol to butyraldehyde via hydride transfer to furfural.

10.1002/cctc.201701866

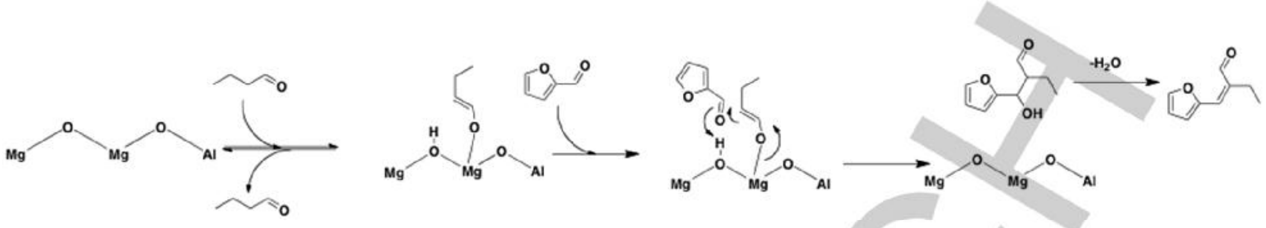

Scheme 5. Proposed mechanism of aldol condensation of butyraldehyde and furfural.

Figure 5 shows the selectivity of the reaction as a function of the butanol conversion (controlled by the residence time). At low butanol conversion values, the main product was butyraldehyde. At higher butanol conversion values, selectivity shifts towards the butyraldehyde-furfural adduct. These observations suggest that butanol is first dehydrogenated to the reactive butyraldehyde, which in turn reacts with furfural to form the adduct.

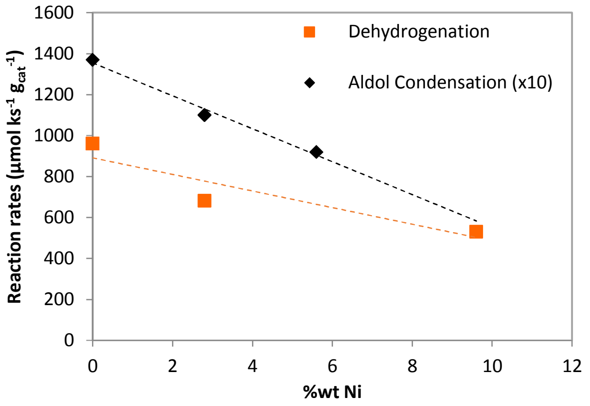

Figure 3. Effects of Ni loading on dehydrogenation and aldol condensation rates. Dashed lines indicate qualitative trends. 413 K, 0.8 kPa furfural, 0.4 kPa butanol.

Comparing the two catalysts under identical reaction conditions (liquid phase, 413 K, Figure 1 and Figure S 1) and a conversion below 25%, we can calculate the turnover frequency over both. Assuming that the (100) plane is the dominant one on the surface of the mixed oxide and using a lattice constant of a = 4.214 Å, there are two oxygen atoms every 17.76 Å^2. Given the surface area of the mixed oxide being equal to 221 m^2 g^{-1}, the number of active sites is 2.3 mmol/g. Based on the reaction rate in the heterogeneous system, the turnover frequency (rate normalized by surface oxygen atoms) is equal to 0.78 h^{-1}, compared to 1.6 h^{-1} in the homogeneous system. This is also comparable to systems reported in the literature[27], such as a Ru/RuOx/C system (3.6 h^{-1})[28] used in the context of furfural hydrodeoxygenation. On a per-site basis, the turnover rates reported herein are lower than those reported over Hf-BEA Lewis acidic zeolites (480 h^{-1}).[29] However, the rate disadvantage of the Mg-Al oxide catalytic system is outweighed by the lower cost and abundance of these materials, compared to Ru and Hf.

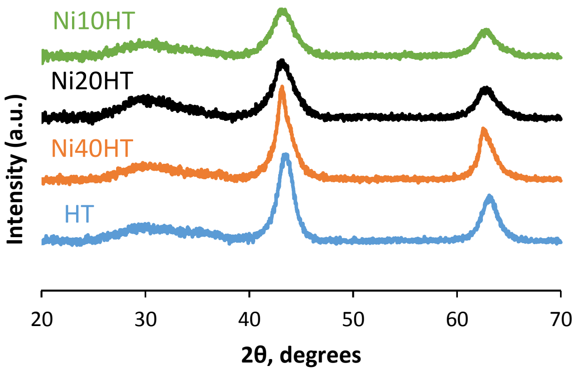

Figure 4. X-ray diffractograms of calcined NiHT catalysts.

Figure 6 shows the dependence of the rate of butanol dehydrogenation on furfural and butanol pressures. As was the case in the liquid phase Ni(dppe)Cl$_2$-catalyzed reaction, the dehydrogenation rate is first-order in furfural. On the other hand, the dependence on butanol pressure shows a first-order dependence at low butanol pressures and is independent of butanol pressure at the higher pressure regime. This behavior can be explained by the change of surface coverage from a clean surface to a butanol covered surface, probably in the form of butoxide, as basic solids are known to dissociatively adsorb alcohols on their surface, forming alkoxides, as has been shown in past XPS[24] and FT-IR investigations.[25]

These observations suggest that furfural participates in the rate-limiting step of the butanol dehydrogenation reaction. This is consistent with a transfer hydrogenation, in which a butoxide on the surface transfers a hydride atom to a molecule of furfural, forming furfuryl alcohol and butyraldehyde. In order to test this hypothesis, we performed kinetic isotope effect experiments, using 1,1-d$_2$-butanol and butanol-OD. No kinetic isotope effect was detected in the case of butanol deuterated in the OH group. However, in the case of the C$_1$ di-deuterated butanol, we measured a KIE equal to 2.0. This is consistent with a primary kinetic isotope effect and is suggestive of a C_1-H bond scission in the rate-determining step. The combination of kinetics and isotope effects supports the hypothesis that the rate-determining step of this sequence is the hydride transfer from the butoxide to the furfural. The reaction sequence for the transfer hydrogenation is shown in scheme 3 and the proposed transition state is shown in scheme 4. These results show that the dehydrogenation of butanol to the reactive butyraldehyde takes place via a similar hydride transfer step from the C_1 carbon of the butanol to that of the furfural.

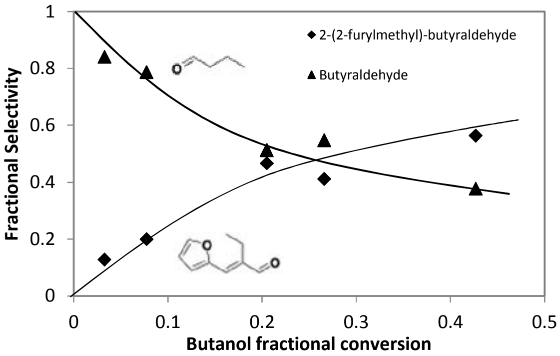

Figure 5. Effects of residence time on the selectivity of the condensation of butanol and furfural. 413 K, 0.8 kPa furfural, 0.4 kPa butanol. The residence time was varied from 0.5 to 4.3 ks kg_{cat} $mol_{butanol}^{-1}$

In the condensation step, we propose that the reaction proceeds through an aldol-type mechanism, in which an enolate (formed from butyraldehyde) attacks the electrophilic carbonyl carbon of the furfural, based on the regioselectivity of the product. The condensation mechanism is shown in scheme 5.

To probe the aldol condensation step of the reaction, we co-fed butyraldehyde and furfural over the catalyst. The rate of aldol condensation was independent of the butyraldehyde pressure, as can be seen in Figure 7. Since the reaction pathway requires the participation of butyraldehyde in every step, this observation shows that butyraldehyde participates in the kinetically relevant step and, at the same time, that it is the most abundant surface intermediate during condensation reactions. It is also noteworthy that the pressure at which butyraldehyde covers the surface completely is much lower (lower than 0.1 kPa) than that for butanol (5 kPa). This is consistent with the observations of Hanspal et al.,[30] who showed that during the ethanol Guerbet reaction, the aldehyde species are bound more strongly to MgO than the alcohol species.

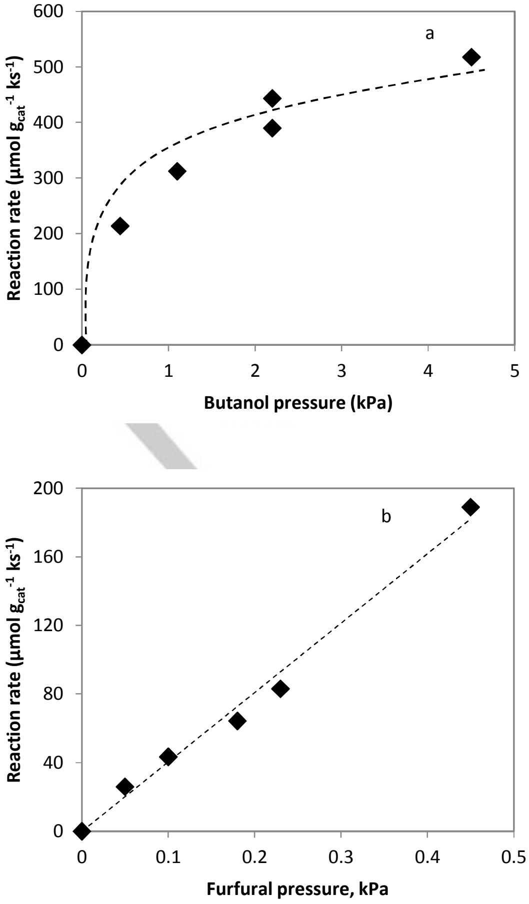

Figure 6. Effects of butanol (a) and furfural pressure (b) on the butanol dehydrogenation rate. (413 K, 0.8 kPa furfural or 1.1 kPa butanol).

We also observe that the aldol condensation rate showed a first-order dependence on the furfural pressure (Figure S 2). This observation enabled us to distinguish between a rate-determining enolate formation step and an equilibrated enolate formation step. In particular, the observation indicates that furfural participates in the rate-determining step of the aldol condensation between furfural and butyraldehyde, signifying an equilibrated enolate formation. This is consistent with the kinetics reported in the literature for the condensation of acetone with butyraldehyde and acetaldehyde.[10c] In this, it was shown that the enolate formation from the acetone is equilibrated with gas-phase acetone. In this case, the observation that furfural participates in the rate-determining step shows that the enolate formation from butyraldehyde is equilibrated and that the C-C bond formation is rate-determining for the condensation of furfural and butyraldehyde.

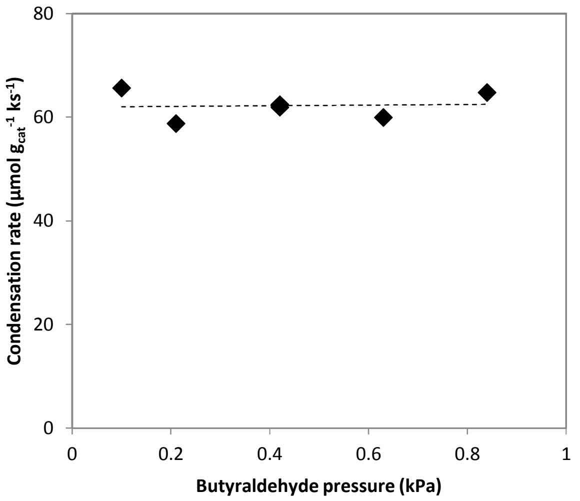

Figure 7. Dependence of aldol condensation rate on butyraldehyde pressure. 413 K, 0.8 kPa furfural, balance He.

Conclusions

In this work, we have shown that the coupling of furfural with aliphatic alcohols proceeds via a transfer hydrogenation-aldol condensation mechanism. The transfer of a hydride from an alkoxide to the furfural is the rate-limiting step in both the homogeneous and heterogeneous cases, as can be shown by kinetic experiments and the kinetic isotope effects. In the heterogeneous system, both the transfer hydrogenation and the aldol condensation are catalyzed by the basic sites on the mixed Mg-Al oxide. On the other hand, in the homogeneous system, the K_2CO_3 base is not strong enough to catalyze the transfer hydrogenation, necessitating the presence of the Ni complex that acts as a Lewis acid to coordinate the furfural and the butoxide and catalyze the hydride transfer.

Experimental Section

[1,3-Bis(diphenylphosphino)ethane]dichloronickel(II) [Hereafter referred to as Ni(dppe)Cl_2] was prepared as follows: $NiCl_2.6H_2O$ (Spectrum Chemical) was dissolved in 20 mL ethanol (Koptec) and was reacted at room temperature for 30 min with a solution of 1,3-bis(diphenylphosphino)ethane (Sigma-Aldrich) in dichloromethane (Spectrum Chemical). The orange-red solid was filtered out, washed with ethanol and dried in the fume hood.

Preparation of Ni-substituted hydrotalcites was carried out by modifying a method described by Climent et al.[31]. Briefly, layered hydroxycarbonates were precipitated from a solution of Ni, Mg and Al nitrates (1.5 M total metal concentration, 3:1 Mg:Al – purchased from Spectrum Chemical Co.) with an equal volume of a NH_4OH and $(NH_4)_2CO_3$ solution (3.375 M and 1 M, respectively – Spectrum Chemical Co.). After precipitation at 333 K, the solids were filtered and washed with copious amounts of warm (323 K) water. The solids were then dried at ambient air at 368 K and calcined at 823 K for 4 h, with a ramp rate of 1 K/min. Catalysts prepared in this manner are labeled NiXXHT, where XX is the Mg:Ni ratio in the catalyst.

The surface areas of the catalysts were measured by nitrogen physisorption at 77 K, using a Micromeritics TriStar 3000 instrument. The surface area was quantified using the instrument software by a fitting the BET equation to the P/P_0 data.

The crystalline phase of the catalysts was determined by X-ray diffraction, using a Bruker D8 Advance X-ray diffractometer, equipped with a Cu Ka source.

Liquid-phase kinetic experiments were performed in 12 mL batch reactors (Qtube, Sigma-Aldrich). In these experiments, the reactants, furfural and butanol were loaded with an appropriate amount of catalyst under air, sealed and heater under stirring to the reaction temperature. After the reaction was complete, the reactor was cooled, the pressure was released and the contents diluted with toluene or THF. The solids were separated and aliquots of the liquid were taken for analysis by GC-MS and GC-FID (Varian 3800, VF-5MS capillary columns).

Gas-phase kinetic experiments were performed in a gas-phase flow reactor setup. Helium and hydrogen gases (Praxair 99.999%) were introduced into the system through mass flow controllers (Parker model 201). Liquid reactants, furfural (Sigma-Aldrich), butanol (Sigma-Aldrich) and butyraldehyde (TCI America), were introduced into the gas stream through syringe pumps (KD Scientific Legato 100). Transfer lines were heated to above 403 K to prevent condensation of reactants and products. The catalyst bed was supported on a borosilicate glass frit in a tubular reactor with plug-flow hydrodynamics. The temperature of the reactor was kept constant at 413-443 K by an electric furnace (APS PA), controlled by a PID controller (Watlow). The reaction products were analyzed by online gas chromatography (Shimadzu GC 2014). Prior to reaction, the catalyst was treated in a 50% H_2/He mixture at 523 K for 1h. Reaction rates were calculated at differential conversion, i.e. lower than 5%. Details on the calculations of the rates can be found in the Supporting Information. The influence of internal and external mass transfer limitations was ruled out. Details for the rate calculation formulae, as well as the calculations for the Mears criterion and the Weisz-Prater criterion, can be found in the Supporting Information.

Acknowledgements

This work was funded by BP through the Energy Biosciences Institute. The authors wish to thank Prof. F. Dean Toste and Dr. Sanil Sreekumar for useful technical discussions, and Mr. Matthew Gilkey and Ms. Huong Nguyen for their insightful edits to the manuscript.

Keywords: Aldol condensation • furfural • kinetics • transfer hydrogenation • hydrotalcite

[1] a. S. Sadula, O. Oesterling, A. Nardone, B. Dinkelacker, B. Saha, *Green Chemistry* **2017**, *19*, 3888-3898; b. S. Caratzoulas, M. E. Davis, R. J. Gorte, R. Gounder, R. F. Lobo, V. Nikolakis, S. I. Sandler, M. A. Snyder, M. Tsapatsis, D. G. Vlachos, *The Journal of Physical Chemistry C* **2014**, *118*, 22815-22833.

[2] a. K. A. Goulas, F. D. Toste, *Current Opinion in Biotechnology* **2016**, *38*, 47-53; b. I. Wheeldon, P. Christopher, H. Blanch, *Current Opinion in Biotechnology* **2017**, *45*, 127-135.
[3] R. Weingarten, A. Rodriguez-Beuerman, F. Cao, J. S. Luterbacher, D. M. Alonso, J. A. Dumesic, G. W. Huber, *ChemCatChem* **2014**, *6*, 2229-2234.
[4] Z. J. Brentzel, K. J. Barnett, K. Huang, C. T. Maravelias, J. A. Dumesic, G. W. Huber, *ChemSusChem* **2017**, *10*, 1351-1355.
[5] a. J. E. Logsdon, in *Kirk-Othmer Encyclopedia of Chemical Technology*, John Wiley & Sons, Inc., **2000**; b. E. M. Green, *Current Opinion in Biotechnology* **2011**, *22*, 337-343.
[6] P. Anbarasan, Z. C. Baer, S. Sreekumar, E. Gross, J. B. Binder, H. W. Blanch, D. S. Clark, F. D. Toste, *Nature* **2012**, *491*, 235-239.
[7] Y. Zhang, X. Chen, J. Luo, B. Qi, Y. Wan, *Bioresource Technology* **2014**, *158*, 396-399.
[8] D. M. Alonso, J. Q. Bond, J. A. Dumesic, *Green Chemistry* **2010**, *12*, 1493-1513.
[9] a. S. Dutta, A. Bohre, W. Zheng, G. R. Jenness, M. Núñez, B. Saha, D. G. Vlachos, *ACS Catalysis* **2017**, *7*, 3905-3915; b. A. Corma, O. de la Torre, M. Renz, N. Villandier, *Angewandte Chemie International Edition* **2011**, *50*, 2375-2378; c. G. Li, N. Li, Z. Wang, C. Li, A. Wang, X. Wang, Y. Cong, T. Zhang, *ChemSusChem* **2012**, *5*, 1958-1966.
[10] a. K. A. Goulas, S. Sreekumar, Y. Song, P. Kharidehal, G. Gunbas, P. J. Dietrich, G. R. Johnson, Y. C. Wang, A. M. Grippo, L. C. Grabow, A. A. Gokhale, F. D. Toste, *Journal of the American Chemical Society* **2016**, *138*, 6805-6812; b. E. R. Sacia, M. Balakrishnan, M. H. Deaner, K. A. Goulas, F. D. Toste, A. T. Bell, *ChemSusChem* **2015**, *8*, 1726-1736; c. K. A. Goulas, G. Gunbas, P. J. Dietrich, S. Sreekumar, A. Grippo, J. P. Chen, A. A. Gokhale, F. D. Toste, *ChemCatChem* **2017**, *9*, 677-684.
[11] a. S. Liu, S. Dutta, W. Zheng, N. S. Gould, Z. Cheng, B. Xu, B. Saha, D. G. Vlachos, *ChemSusChem* **2017**, *10*, 3225-3234; b. S. Dutta, B. Saha, *ACS Catalysis* **2017**, *7*, 5491-5499.
[12] a. J. Cueto, L. Faba, E. Díaz, S. Ordóñez, *Applied Catalysis B: Environmental* **2017**, *201*, 221-231; b. M. Kim, J. Park, H. P. R. Kannapu, Y.-W. Suh, *Catalysts* **2017**, *7*, 249; c. S. Li, F. Chen, N. Li, W. Wang, X. Sheng, A. Wang, Y. Cong, X. Wang, T. Zhang, *ChemSusChem* **2017**, *10*, 711-719.
[13] a. J. Cueto, L. Faba, E. Díaz, S. Ordóñez, *ChemCatChem* **2017**, *9*, 1765-1770; b. J. Yang, S. Li, N. Li, W. Wang, A. Wang, T. Zhang, Y. Cong, X. Wang, G. W. Huber, *Industrial & Engineering Chemistry Research* **2015**, *54*, 11825-11837.
[14] a. J. Xu, N. Li, X. Yang, G. Li, A. Wang, Y. Cong, X. Wang, T. Zhang, *ACS Catalysis* **2017**, *7*, 5880-5886; b. W. Wang, N. Li, S. Li, G. Li, F. Chen, X. Sheng, A. Wang, X. Wang, Y. Cong, T. Zhang, *Green Chemistry* **2016**, *18*, 1218-1223.
[15] L. Faba, E. Díaz, A. Vega, S. Ordóñez, *Catalysis Today* **2016**, *269*, 132-139.
[16] M. Koehle, E. Saraçi, P. Dauenhauer, R. F. Lobo, *ChemSusChem* **2017**, *10*, 91-98.
[17] D. S. Park, K. E. Joseph, M. Koehle, C. Krumm, L. Ren, J. N. Damen, M. H. Shete, H. S. Lee, X. Zuo, B. Lee, W. Fan, D. G. Vlachos, R. F. Lobo, M. Tsapatsis, P. J. Dauenhauer, *ACS Central Science* **2016**, *2*, 820-824.
[18] S. Sreekumar, M. Balakrishnan, K. Goulas, G. Gunbas, A. A. Gokhale, L. Louie, A. Grippo, C. D. Scown, A. T. Bell, F. D. Toste, *ChemSusChem* **2015**, *8*, 2609-2614.
[19] G. M. Strunz, C.-M. Yu, *Canadian Journal of Chemistry* **1988**, *66*, 1081-1083.
[20] a. G. Moineau, M. Minet, P. Dubois, P. Teyssié, T. Senninger, R. Jérôme, *Macromolecules* **1999**, *32*, 27-35; b. C. Granel, P. Dubois, R. Jérôme, P. Teyssié, *Macromolecules* **1996**, *29*, 8576-8582.
[21] a. F. Shi, M. K. Tse, X. Cui, D. Gördes, D. Michalik, K. Thurow, Y. Deng, M. Beller, *Angewandte Chemie International Edition* **2009**, *48*, 5912-5915; b. C. Li, H. Kawada, X. Sun, H. Xu, Y. Yoneyama, N. Tsubaki, *ChemCatChem* **2011**, *3*, 684-689.
[22] a. D. A. Evans, S. J. Miller, T. Lectka, P. von Matt, *Journal of the American Chemical Society* **1999**, *121*, 7559-7573; b. K. Shuji, A. Kenji, Y. Hidetoshi, W. Eiji, *Bulletin of the Chemical Society of Japan* **2000**, *73*, 681-687.
[23] W. Gerlach, *Zeitschrift für Physik* **1922**, *9*, 184-192.
[24] a. F. Millange, R. I. Walton, D. O'Hare, *Journal of Materials Chemistry* **2000**, *10*, 1713-1720; b. J. Pérez-Ramírez, S. Abelló, N. M. van der Pers, *Chemistry – A European Journal* **2007**, *13*, 870-878.
[25] R. Debek, M. Motak, D. Duraczyska, F. Launay, M. E. Galvez, T. Grzybek, P. Da Costa, *Catalysis Science & Technology* **2016**, *6*, 6705-6715.
[26] a. P. S. Kumbhar, J. Sanchez-Valente, J. Lopez, F. Figueras, *Chemical Communications* **1998**, 535-536; b. J. R. Ruiz, C. Jiménez-Sanchidrián, J. M. Hidalgo, J. M. Marinas, *Journal of Molecular Catalysis A: Chemical* **2006**, *246*, 190-194; c. Y. Zhu, S. Liu, S. Jaenicke, G. Chuah, *Catalysis Today* **2004**, *97*, 249-255.
[27] M. J. Gilkey, B. Xu, *ACS Catalysis* **2016**, *6*, 1420-1436.
[28] a. P. Panagiotopoulou, D. G. Vlachos, *Applied Catalysis A: General* **2014**, *480*, 17-24; b. M. J. Gilkey, P. Panagiotopoulou, A. V. Mironenko, G. R. Jenness, D. G. Vlachos, B. Xu, *ACS Catalysis* **2015**, *5*, 3988-3994.
[29] M. Koehle, R. F. Lobo. *Catal. Sci. Technol.* **2016**, *6*, 3018-3026.
[30] S. Hanspal, Z. D. Young, H. Shou, R. J. Davis, *ACS Catalysis* **2015**, *5*, 1737-1746.
[31] M. J. Climent, A. Corma, S. Iborra, A. Velty, *Journal of Catalysis* **2004**, *221*, 474-482.

Entry for the Table of Contents

FULL PAPER

We investigate the tandem dehydrogenation and aldol condensation between furfural and butanol to jet fuel precursors. We establish that heterogeneous systems are equally active with homogeneous ones, with the rate-determining step being a hydride transfer from butanol to furfural.

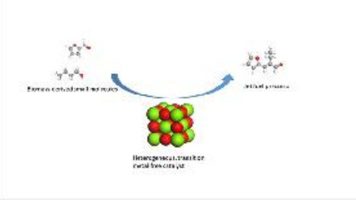

Konstantinos A. Goulas, Amit A. Gokhale*

Page No. – Page No.

Kinetics of the Homogeneous and Heterogeneous Coupling of Furfural with Biomass-derived Alcohols